The Plant Cell, Vol. 6, 333–349, March 1994 © 1994 American Society of Plant Physiologists

Homeotic Transformation of Ovules into Carpel-like Structures in Arabidopsis

Zora Modrusan,[a] Leonore Reiser,[b] Kenneth A. Feldmann,[c] Robert L. Fischer,[b] and George W. Haughn[a,1]

[a] Botany Department, University of British Columbia, Vancouver, British Columbia, V6T 1Z4, Canada
[b] Department of Plant Biology, University of California, Berkeley, California 94720
[c] Department of Plant Sciences, University of Arizona, Tucson, Arizona 85721

Ovules are specialized reproductive organs that develop within the carpels of higher plants. In Arabidopsis, mutations in two genes, *BELL1* (*BEL1*) and *APETALA2* (*AP2*), disrupt ovule development. In Bel1 ovules, the inner integument fails to form, the outer integument develops abnormally, and the embryo sac arrests at a late stage of megagametogenesis. During later stages of ovule development, cells of the outer integument of a Bel1 ovule sometimes develop into a carpel-like structure with stigmatic papillae and second-order ovules. The frequency of carpel-like structures was highest when plants were grown under conditions that normally induced flowering and was correlated with ectopic expression in the ovule of *AGAMOUS* (*AG*), an organ-identity gene required for carpel formation. Together, these results suggested that *BEL1* negatively regulates *AG* late in ovule development. Likewise, mutants homozygous for the strong *AP2* allele *ap2-6* sometimes displayed structures with carpel-like features in place of ovules. However, such abnormal Ap2 ovules are much less ovulelike in morphology and form earlier than the Bel1 carpel-like structures. Because one role of the *AP2* gene is to negatively regulate *AG* expression early in flower development, it is possible that *AP2* works in a similar manner in the ovule. A novel ovule phenotype observed in Bel1/Ap2-6 double mutants suggested that *BEL1* and *AP2* genes function independently during ovule development.

INTRODUCTION

Ovules, located within the carpels of flowering plants, generate the female gametophyte, mediate fertilization processes, and support the development of the embryo. The morphology, histology, and ultrastructure of angiosperm ovules have been characterized in a large number of species, including Arabidopsis (Misra, 1962; Webb and Gunning, 1990, 1991; Guignard et al., 1991; Mansfield and Briarty, 1991; Mansfield et al., 1991; Robinson-Beers et al., 1992; Modrusan et al., 1994a). Typically, the angiosperm ovule consists of a nucellus (megasporangium) enclosed by integuments and connected to the ovary wall by a funiculus. The female gametophyte or embryo sac develops within the nucellus from an archesporial cell that gives rise to a linear tetrad of haploid megaspores. In Arabidopsis, only one megaspore enters megagametogenesis to produce a seven-celled, eight-nucleate embryo sac.

The ovule is a substructure of a carpel. Carpel development is known to be specified by the class C organ-identity genes (for a review, see Coen and Meyerowitz, 1991). In Arabidopsis, only a single class C gene, *AGAMOUS* (*AG*), has been identified. Loss-of-function mutations in *AG* are associated with the inability to develop carpels (Bowman et al., 1989), whereas the ectopic expression of *AG* can direct both floral organ primordia (Drews et al., 1991) and ovule primordia (Mandel et al., 1992) to develop as carpel-like structures. Besides class C genes controlling ovule development, one would expect that additional genes are required for specific aspects of ovule morphogenesis. Two genes that may specifically regulate ovule morphogenesis are *BELL1* (*BEL1*) and *SHORT INTEGUMENTS* (*SIN1*). They have recently been identified by mutation (Robinson-Beers et al., 1992; Modrusan et al., 1994b).

Here, we provide analysis of two new *BEL1* alleles and an allele of *APETALA2* (*AP2*), a gene that antagonizes *AG* gene expression during floral development (Drews et al., 1991). All of these mutations resulted in a transformation of ovules into structures resembling carpels. Our results provided evidence that *BEL1* and *AP2* play important, distinct roles in ovule development, acting either directly or indirectly to suppress alternative developmental programs within the ovule.

RESULTS

Isolation and Genetic Analysis of New *bel1* Alleles

To isolate mutations that affect ovule development, ~8000 Arabidopsis (Wassilewskija ecotype) lines transformed with the T-DNA of Agrobacterium (Feldmann, 1991) were screened for

[1] To whom correspondence should be addressed.

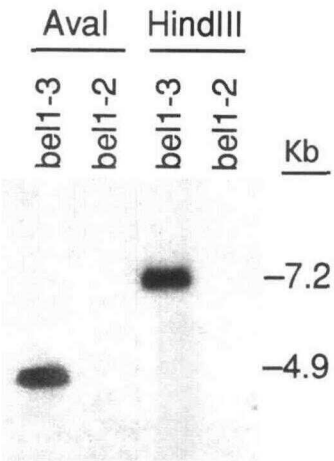

Figure 1. DNA Gel Blot of Bel1-2 and Bel1-3 Mutants.

DNA was isolated from Bel1-2 and Bel1-3 mutant plants, digested with AvaI or HindIII, blotted, and hybridized with an *NPTII* probe. The length of the fragments is indicated at right in kilobases.

mutations that reduce fertility on the basis of reduced silique size. Female-sterile mutants were identified using reciprocal crosses with the wild type. Siliques from these female-sterile mutants were then dissected to identify possible abnormalities in ovule development. Two lines, designated female-sterile (Fms1) and fruitless (Fts1), had similar phenotypes, as described in detail below.

To determine the genetic basis of the mutant phenotypes, both Fms1 and Fts1 mutants were used as a male parent in a cross to a wild-type plant. All of the F_1 progeny examined had the fertile wild-type phenotype. F_2 progeny from the cross with Fms1 yielded 1569 fertile and 570 sterile plants (3:1, $\chi^2 = 3.0981$, $P > 0.05$). F_2 progeny from the cross with Fts1 yielded 2324 fertile and 748 sterile plants (3:1, $\chi^2 = 0.6944$, $P > 0.1$). These results indicated that both sterile Fms1 and Fts1 phenotypes are due to single recessive nuclear mutations.

An allelism test was performed to determine if the Fms and Fts phenotypes are the result of mutations in the same gene. Reciprocal crosses involving a male parent homozygous for one mutation and a female parent heterozygous for the other mutation were performed. The F_1 progeny from *FTS/fts* × *fms/fms* were 42 fertile to 38 sterile (1:1, $\chi^2 = 0.2$, $P > 0.5$), whereas the F_1 progeny from *FMS/fms* × *fts/fts* were 88 fertile to 87 sterile (1:1, $\chi^2 = 0.005$, $P > 0.9$). These results indicated that *fms1* and *fts1* are alleles. In addition, a previously described female-sterile mutant generated by ethyl methanesulfonate mutagenesis, designated Bel1, has a phenotype similar to the Fms1 and Fts1 mutants (Robinson-Beers et al., 1992). To determine the genetic relationship between Bel1 and Fms1, we crossed female *BEL1/bel1* × *fms/fms* male. Among 35 F_1 progeny tested, 19 were fertile and 16 were sterile (1:1, $\chi^2 = 0.26$, $P > 0.8$), indicating that *bel1* and *fms1* represent different alleles of the same genetic locus. For this reason, we designated *fms1* and *fts1* as *bel1-2* and *bel1-3*, respectively.

Bel1-2 and Bel1-3 mutant lines were generated at different times and through separate transformation experiments (Feldmann, 1991); thus, they must represent unique mutational events at the same locus. This conclusion is supported by two lines of evidence. First, kanamycin resistance encoded by the neomycin phosphotransferase II (*NPTII*) gene of the T-DNA cosegregates with the *bel1-3* but not with the *bel1-2* allele (data not shown). Second, as shown in Figure 1, the *NPTII* probe detected a restriction fragment of the size expected for an intact *NPTII* locus (Velten and Schell, 1985) in Bel1-3 but not in Bel1-2 mutant plants.

The map position of the *BEL1* gene was determined by genetic crosses to marker lines. Data from 189 F_2 progeny obtained from the cross Bel1-3 × W100 (Koornneef et al., 1987) indicated that the *BEL1* was genetically linked to the marker *transparent testa* (*tt3*) located on chromosome 5 (data not shown). A more accurate map position for the *BEL1* gene was obtained by analyzing F_2 progeny from the cross Bel1-3 × TC35, a line carrying three genetic markers, *ttg*, *pgm*, and *yi*, on chromosome 5. Analysis of F_2 progeny (749) indicated linkage of *BEL1* to *TTG* (23.24 ± 3.4 map units) and to *PGM* (19.52 ± 3.4 map units). Figure 2 illustrates the chromosomal position of *BEL1* with respect to the current linkage map of Arabidopsis.

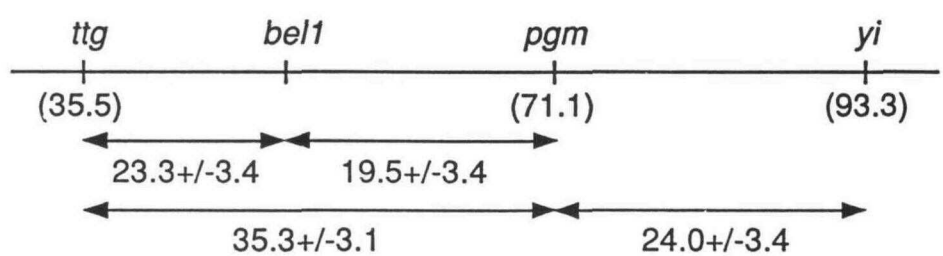

Figure 2. Position of *BEL1* on Chromosome 5 of Arabidopsis.

Arrows span distances between genetic markers, and the numbers beneath the arrows represent distance and SE in map units. Distances have not been corrected for double crossovers. Numbers in parentheses represent the chromosomal location of the markers from the current linkage map of Arabidopsis.

Wild-Type Ovule Development

We analyzed the ontogeny, morphology, and anatomy of wild-type ovules to serve as a basis for comparison to mutant ovules and to correlate ovule development with other events in floral development. Figures 3 and 4 show the results. Stage 8 of Arabidopsis flower development is characterized by the formation of an open gynoecial cylinder (Figure 3A; Smyth et al., 1990). At this time, four files of ovule primordia are initiated, two from each of the placental tissues located at the carpel margins (Figure 3B). Ovule primordia initiate asynchronously; initiation starts in the lower part and progresses toward the opening of the gynoecial cylinder. Later events in ovule development appear to be more synchronous. The gynoecial cylinder continues to grow as an open tube, although its apex becomes tapered (Figure 3D, stage 9). The central septum forms and divides the cylinder into two locules, and the two files of enlarging ovule primordia in each locule display an interlocking pattern (Figure 3E). Within each primordium, the megasporocyte is recognizable by its size and can be found directly below the apex of the nucellus (Figure 4A).

Complete closure of the gynoecial cylinder at the top and the appearance of immature papilla cells indicate the beginning of stage 10 (Figure 3G). Initiation of the inner integument occurs in stage 10 ovules marked by the cell outgrowth at the base of the nucellar region (Figure 3H). As the stigmatic papillae develop at the tip of the gynoecium (Figure 3J, stage 11), the nucellus and funiculus can easily be distinguished on the basis of both morphology and cell surface features and are separated by two rings of tissue comprising the inner and outer integument primordia (Figure 3K). Within the nucellus, the megasporocyte enters meiosis (Figure 4C).

By stage 12, megasporogenesis has resulted in the formation of a linear tetrad in which only the chalazal megaspore survives (Figure 4E). During the same period, both integuments exhibit intensive growth that can be divided into substages. In early stage 12, the outer integument grows asymmetrically through increased cell divisions on the side facing the central septum (Figure 3N). Growth of the inner and outer integuments continues upward, enclosing the nucellus (Figure 3O). The nucellus changes its orientation with respect to the funiculus from being parallel to being perpendicular (anatropous ovule). Growth of the integuments contributes to ovule enlargement. Concurrently, the ovary expands, the stylar region elongates, and typical style cells differentiate below the stigmatic papillae (Figure 3M).

At ovule maturity (stage 13), the gynoecium possesses well-differentiated stigmatic papillae, style, and ovaries (Figure 3R). The outer integument completely overgrows the inner integument, forming the micropylar opening (Figure 3S). The nucellus degenerates, and the embryo sac is appressed by a newly differentiated cell layer of the inner integument, the endothelium. Within the embryo sac, megagametogenesis is completed with the formation of a seven-celled, eight-nucleate female gametophyte (Figure 4G). No obvious morphological changes of gynoecium and unfertilized ovules occurred after stage 13.

The aforementioned results are in agreement with previous studies of Arabidopsis ovule development (Misra, 1962; Webb and Gunning, 1990, 1991; Guignard et al., 1991; Mansfield and Briarty, 1991; Mansfield et al., 1991; Robinson-Beers et al., 1992; Modrusan et al., 1994a), extend previous observations to include events at the time of ovule primordia initiation, and correlate wild-type ovule development with other aspects of floral ontogeny (Smyth et al., 1990).

Bel1 Mutant Ovule Development

As with the wild type, the ontogeny, morphology, and anatomy of Bel1 ovules were analyzed using light microscopy and scanning electron microscopy. The results are shown in Figures 3 and 4 and summarized in Table 1. Relative to the wild type, Bel1 ovules do not show any deviation during early stages (8 and 9) of development. Bel1 ovule primordia are initiated from the placental tissue (Figure 3C) and enlarge (Figure 3F) at the same time and in the same place as the wild type. Concomitantly, the Bel1 megasporocyte below the apex of the nucellus differentiates (Figure 4B).

Differences between Bel1 and wild-type ovule morphogenesis are first discernible at inner integument initiation (stage 10). No structural changes were observed at the expected position of the inner integument primordium, suggesting that the inner integument is not initiated. A single outgrowth, represented by a disorganized cluster of cells, arises at a time and position corresponding to that of the wild-type outer integument primordium (Figure 3I). By stage 11, the putative outer integument primordium enlarges and generates an irregular collar of tissue at the base of the nucellus in Bel1 ovules (Figures 3L and 4D). Asymmetric growth of the collar of tissue forms individual protuberances by stage 12 of Bel1 ovule development (Figure 3P). These meristematic cell outgrowths surround the nucellus, generating an integument-like structure (Figures 3Q and 4F). Stage 13 Bel1 ovules have a distinct morphology because the integument-like structure surrounds but does not enclose the nucellus (Figure 3T). Moreover, the Bel1 integument-like structure also differs in anatomy when compared to the wild-type integuments. For example, the cells of the Bel1 integument-like structure remain densely cytoplasmic and are not as vacuolated as many of the wild-type integument cells.

Embryo sac development is also affected in Bel1 mutant ovules. Development of the female gametophyte of Bel1 ovules proceeds as it did in wild-type ovules, with the formation of the linear tetrad of megaspores (Figure 4F). Shortly afterward, however, embryo sac development is arrested and results in a reduced number of postmitotic cells and remnants of degenerated megaspores (Figure 4H).

At maturity, Bel1 ovules show an orthotropous rather than anatropous orientation. Pollen tubes were often observed

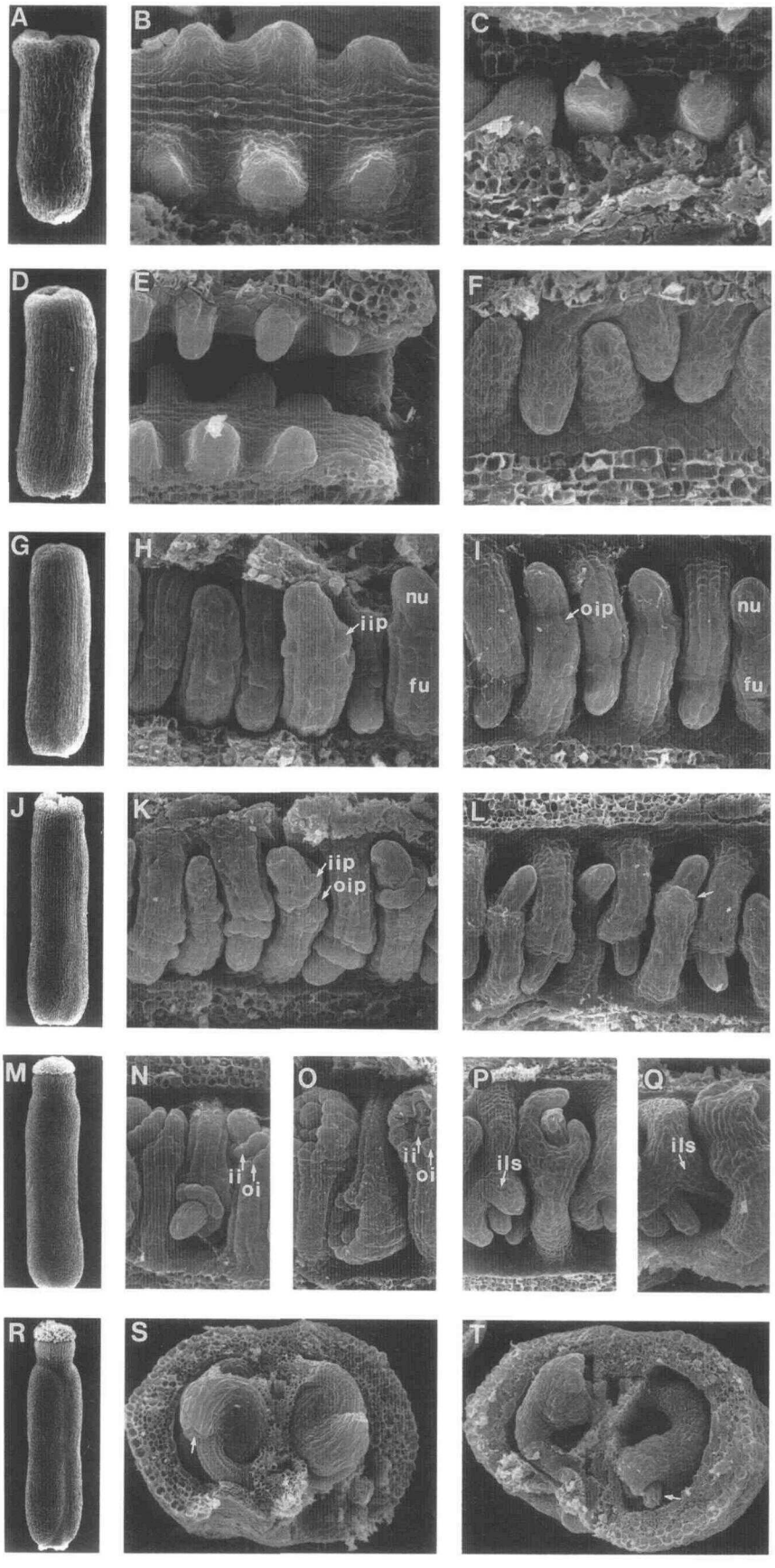
A
B
C
D
E
F
G
H
nu
iip
fu
I
oip
nu
fu
J
K
iip
oip
L
M
N
ii
oi
O
ii
oi
P
ils
Q
ils
R
S
T

surrounding the Bel1 ovules of mature flowers (Figure 5A). This suggested that pollination and pollen tube growth into the ovary are not affected by the absence of functional ovules. Further steps in fertilization usually do not occur; however, of the hundreds of mutant siliques examined, several contained a few viable seeds with abnormal seed coat morphology. The presence of seed indicated that fertilization may occur in rare cases.

Bel1 Ovules Develop Carpel-like Structures

During stage 17 of wild-type flower development, floral organs senesce and abscise, and unfertilized ovules degenerate. Figure 5 shows that Bel1 ovules can have one of two different fates. Most Bel1 ovules, like the unfertilized wild-type ovules, degenerate (Figure 5A). However, in some Bel1 ovules, cells from the region of the integument-like structure continue to grow and differentiate into a structure with carpel-like morphology (Figure 5B) and cell types (Figure 5C). In some cases, second-order mutant ovules are produced along the margins of the carpel-like structure (Figure 5D). Although not previously described (Robinson-Beers et al., 1992), carpel-like structures were also detected in plants homozygous for the *bel1-1* mutant allele (data not shown). In all cases, the carpel-like structures eventually degenerated.

Frequency of Carpel-like Structures Is Influenced by Genetic Background and Growth Conditions

As shown in Table 2, growth conditions and genetic background influenced the frequency of the carpel-like structures. In the Wassilewskija ecotype, under standard growth conditions (continuous light and 22°C), 63% of the *bel1-3* homozygous plants displayed carpel-like structures, with one to two carpel-like structures observed per silique (294 carpel-like structures per 228 siliques). In contrast, carpel-like structures were not observed in the Wassilewskija ecotype when plants were grown at 16°C or when the daylength was reduced from 24 to 10 hr or 16 hr. The frequency of carpel-like structure formation was found to differ in F_2 populations generated by crossing Bel1-3 to wild-type plants of ecotypes Landsberg *erecta* and Columbia. The most dramatic increase in frequency was observed in the outcross to Landsberg *erecta*, in which 90% of the F_2 plants homozygous for *bel1-3* displayed carpel-like structures under standard growth conditions, and as many as 10 carpel-like structures were observed per silique (Table 2; Figure 5E). In all ecotypes tested, reducing the temperature or daylength

Figure 3. Scanning Electron Micrographs of Developing Wild-Type and Bel1 Ovules and Corresponding Gynoecial Morphology from Stage 8 to Stage 13 of Flower Development.

Structures have been given the following abbreviations: nucellus, nu; funiculus, fu; inner integument primordium, iip; outer integument primordium, oip; inner integument, ii; outer integument, oi; integument-like structure, ils.

(A) Open gynoecial cylinder of a stage 8 wild-type flower. Magnification ×180.

(B) Single carpel of the gynoecial cylinder of a stage 8 wild-type flower. Two files of ovule primordia are initiated along carpel margins. Magnification ×845.

(C) Ovule primordia within the dissected gynoecial cylinder of a stage 8 Bel1 flower. Magnification ×543.

(D) Constricted gynoecial cylinder of a stage 9 wild-type flower. Magnification ×106.

(E) Side view into the gynoecial cylinder of a stage 9 wild-type flower. Note the staggered arrangement of enlarged ovule primordia. Magnification ×516.

(F) Enlarged ovule primordia within the gynoecial cylinder of a stage 9 Bel1 flower. Magnification ×591.

(G) Closed gynoecial cylinder of a stage 10 wild-type flower. Magnification ×84.

(H) Elongated ovule primordia within the gynoecial cylinder of a stage 10 wild-type flower. Primordia differentiate into funiculus and nucellus. The arrow indicates initiation of the inner integument primordium. Magnification ×616.

(I) Ovule primordia within the gynoecial cylinder of a stage 10 Bel1 flower. The nucellus and funiculus have differentiated. The arrow indicates initiation of an outer integument. Magnification ×397.

(J) Gynoecium with stigmatic papillae of a stage 11 wild-type flower. Magnification ×76.

(K) Developing ovules within the gynoecium of a stage 11 wild-type flower. Arrows indicate the inner and outer integument primordia at the base of nucellus. Magnification ×413.

(L) Developing ovules within the gynoecium of a stage 11 Bel1 flower. The arrow indicates collar tissue at the base of the nucellus. Magnification ×277.

(M) Gynoecium with well-developed stigmatic papillae and style of a stage 12 wild-type flower. Magnification ×53.

(N) and **(O)** Ovules within the gynoecium of a stage 12 wild-type flower. Arrows indicate the inner and outer integuments enclosing the nucellus. Magnification ×409 for **(N)** and ×344 for **(O)**.

(P) and **(Q)** Ovules within the gynoecium of a stage 12 Bel1 flower. Arrows indicate integument-like structure around the nucellus. Magnification ×207 for **(P)** and ×233 for **(Q)**.

(R) Fully developed gynoecium with stigmatic papillae, style, and ovaries of a stage 13 wild-type flower. Magnification ×39.

(S) Mature ovules within the gynoecium of stage 13 wild-type flower. The arrow indicates micropylar opening. Magnification ×155.

(T) Ovules within the gynoecium of a stage 13 Bel1 flower. The arrow indicates the nucellus, which is not completely enclosed by integument-like structures. Magnification ×169.

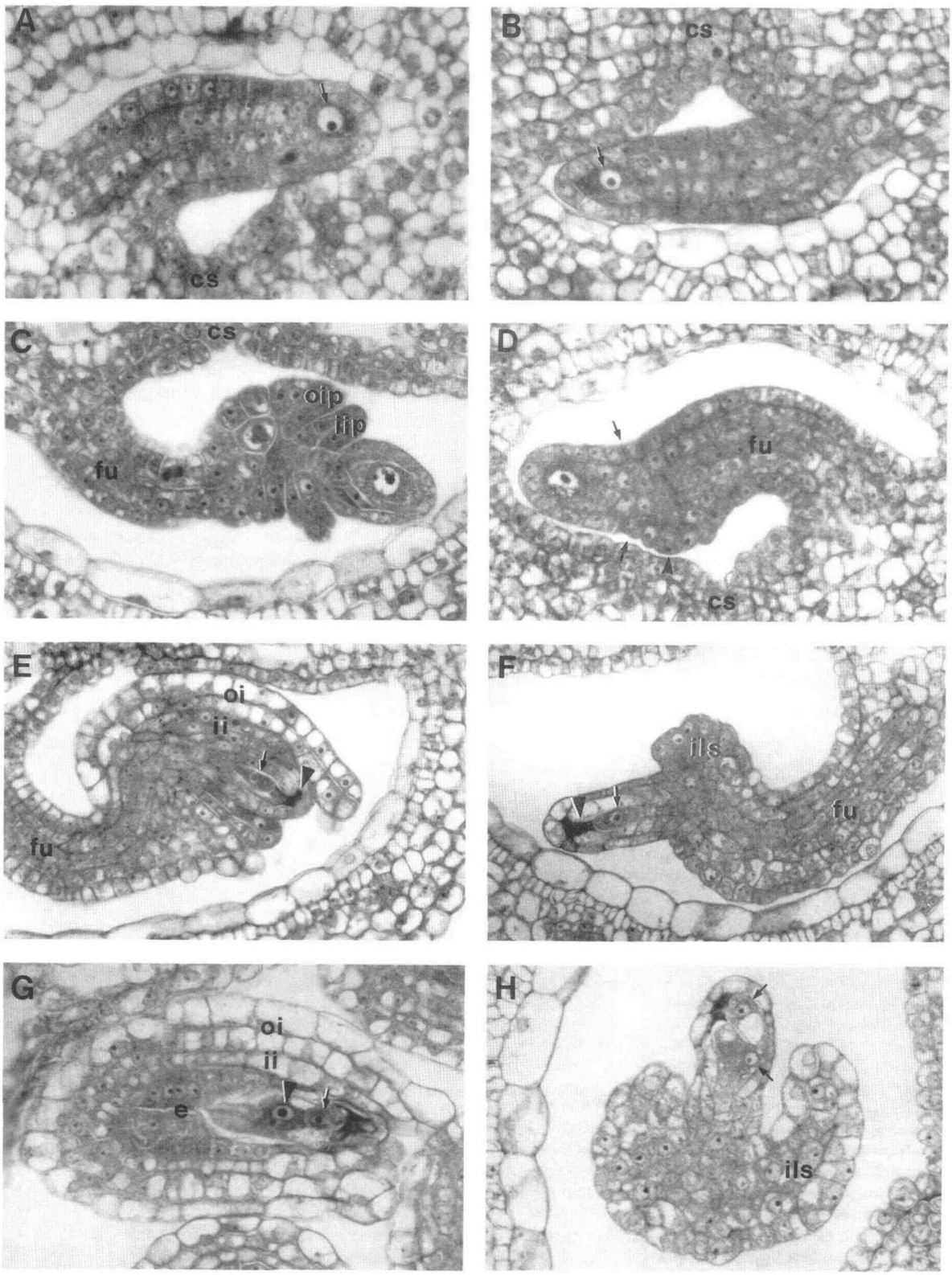

Figure 4. Light Micrographs of Developing Wild-Type and Bel1 Ovules.

Table 1. Wild-Type and Bel1 Ovule Development

		Wild Type		Bel1	
Stage	Morphology of Gynoecium	Ovule	Gametophyte	Ovule	Gametophyte
8	Open cylinder (60–80 μm)	Ovule primordia initiation		NC[a]	NC
9	Cylinder constricted at apex (300 μm)	Ovule primordia enlarge	Megasporocyte visible	NC	NC
10	Closed cylinder (350 μm)	Integument primordia formed	Meiosis begins	Single collar of cells forms below the nucellus	NC
11	Stigmatic papillae develop (425–550 μm)	Integument primordia growth	Meiosis completed	Proliferation of collar cells	NC
12	Style develops (650–850 μm)	Integuments overgrow nucellus	Megagametogenesis	Integument-like structure develops	Embryo sac development arrests
13	Fully formed gynoecium with stigma, style, ovaries (950 μm)	Integument development complete, micropyle formed	Mature embryo sac	Continued growth of integument-like structure	Absence of functional embryo sac
17	Green silique (>7 mm)	Seed coat formation	Embryogenesis	Carpel-like structures form occasionally	

[a] NC, no change from the wild type.

also reduced the frequency of carpel-like structure formation (Table 2).

Mutations in *BEL1* Affect Inflorescence Termination

In addition to the ovule defects, both Bel1-2 and Bel1-3 inflorescences often terminate in carpelloid organs that are commonly fused in a pistil-like structure (data not shown). These pistil-like structures do not seem to result in early termination of the inflorescence because the number of nodes produced by Bel1-3 primary shoots is not significantly different from that of the wild type.

Mutations in *AP2* Result in Carpelloid Ovules

Recessive mutations in the *AP2* gene cause homeotic transformation of perianth organs to reproductive organs and stamens to carpels, a reduction in organ number in the first three whorls, and abnormalities in gynoecial morphology (Komaki et al., 1988; Kunst et al., 1989; Bowman et al., 1991b; E. Schultz, Z. Modrusan, and G.W. Haughn). As shown in Figure 5F, the gynoecium of the Ap2-6 flower contains morphologically normal ovules, thin filaments, and organlike structures with both carpel and sepal characteristics (carpel–sepal ovules) analogous to the sepal–carpel organs of the outermost floral whorl of the Ap2-6 flower (Kunst et al., 1989).

Figure 4. (continued).

Structures have been given the following abbreviations: central septum, cs; funiculus, fu; inner integument primordium, iip; outer integument primordium, oip; inner integument, ii; outer integument, oi; integument-like structure, ils; endothelium, e.

(A) Ovule primordium of a stage 9 wild-type flower. The arrow indicates the megasporocyte. Magnification ×1400.

(B) Ovule primordium of a stage 9 Bel1 flower. The arrow indicates the megasporocyte. Magnification ×2120.

(C) Developing ovule of a stage 11 wild-type flower. The inner and outer integument primordia have been initiated. The premeiotic megasporocyte is apparent within the nucellus. Magnification ×1720.

(D) Developing ovule of a stage 11 Bel1 flower. Arrows indicate the position where the inner integument primordium is expected to form; the arrowhead indicates the collar tissue at the position of the outer integument primordium. Magnification ×1840.

(E) Median section of the ovule of a stage 12 wild-type flower. The arrowhead indicates densely staining cells of the linear tetrad that are degenerating; the arrow indicates the surviving chalazal megaspore. Magnification ×1500.

(F) Ovule with integument-like structure of a stage 12 Bel1 flower. The arrowhead and arrow indicate degenerating cells of the linear tetrad and surviving chalazal megaspore, respectively. Magnification ×1880.

(G) Oblique section through the mature ovule of stage 13 wild-type flower. The arrow indicates the egg cell in contact with synergids; the arrowhead indicates the polar nuclei. Antipodal cells are not visible in this section. Magnification ×1760.

(H) Ovule of a stage 13 Bel1 flower. Arrows indicate two postmitotic cells representing the two-nucleate embryo sac. Magnification ×2120.

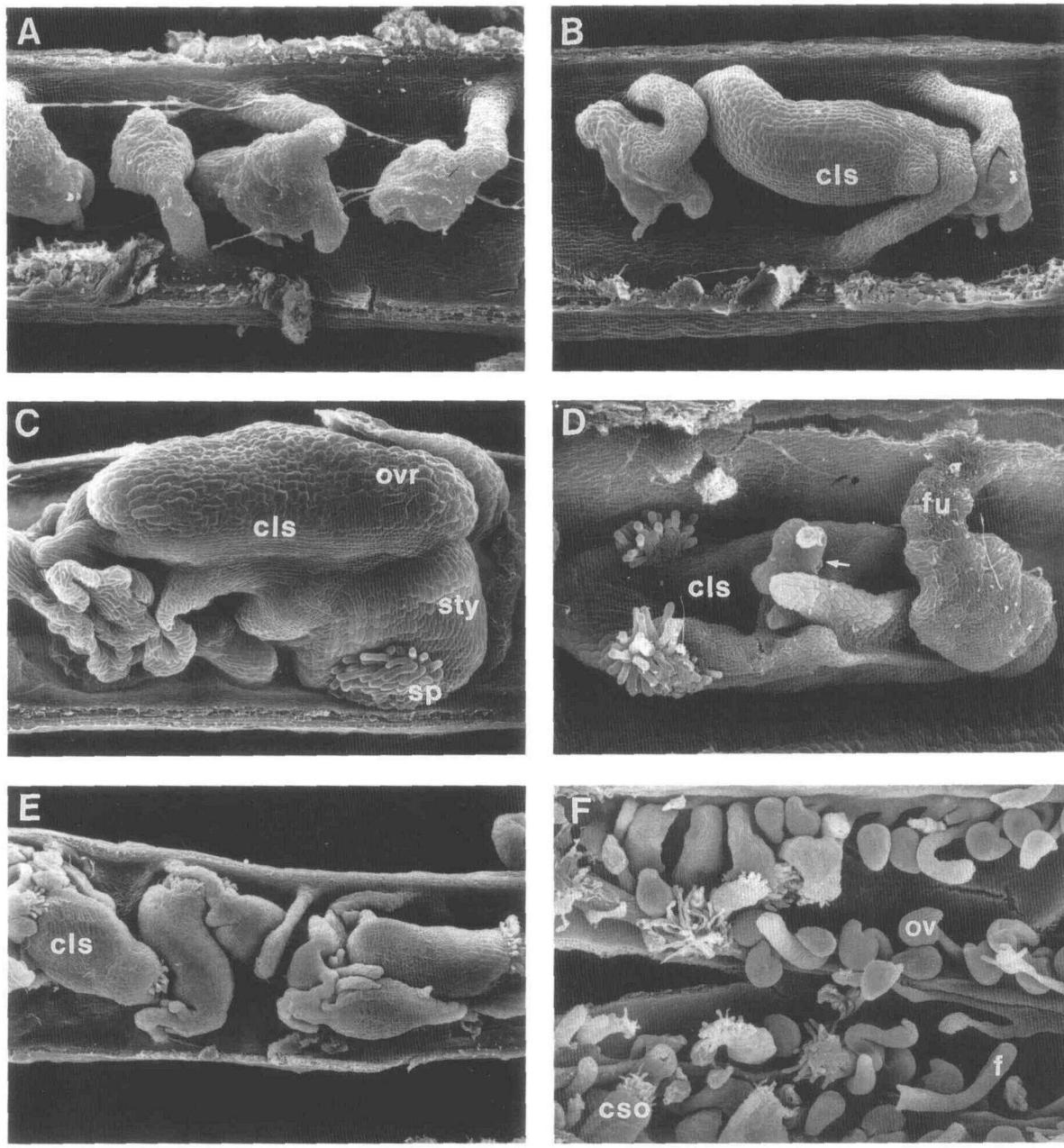

Figure 5. Carpel-like Structures and Carpel–Sepal Ovules in Bel1 and Ap2-6 Mutant Siliques, Respectively.

(A) Dissected stage 17 mutant silique containing degenerating Bel1 ovules. Magnification ×147.

(B) Stage 17 Bel1 ovule developing into carpel-like structure (cls) while two adjacent ovules are degenerating. Magnification ×147.

(C) Developed carpel-like structure (cls) within a stage 17 Bel1 mutant silique. Cell types characteristic of the carpel, including stigmatic papillar (sp), stylar (sty), and ovarian (ovr) cells, have differentiated. Magnification ×115.

(D) Carpel-like structure (cls) attached to the placenta by a funiculus (fu) within a stage 17 Bel1 mutant silique. The arrow indicates a newly initiated ovule on the carpel-like structure. Magnification ×122.

(E) Dissected stage 17 Bel1 silique from a population segregating for Wassilewskija and Landsberg *erecta* genetic backgrounds. Numerous Bel1 carpel-like structures (cls) can be observed. Magnification ×59.

(F) Dissected gynoecium of a stage 13 Ap2-6 mutant flower containing morphologically normal ovules (ov), carpel–sepal ovules (cso), and filaments (f). Magnification ×50.

Table 2. Effects of Growing Conditions and Genetic Background on the Percentage of Plants Having Carpel-like Structures in Stage 17 Siliques

Temperature	Daylength (Light/Dark Hr)	Genetic Background[a] WS	F_2 WS × Col	F_2 WS × Ler
22°C	24	63 (146)	50 (32)	90 (97)
16°C	24	0 (38)	15 (21)	70 (45)
22°C	10/14	0 (25)	0 (05)	0 (22)
22°C	16/8	0 (33)	ND	ND

[a] WS, Wassilewskija; Col, Columbia; Ler, Landsberg *erecta*. Numbers within parentheses indicate the total number of plants examined. Four siliques per plant were analyzed. ND, not determined.

The carpel–sepal and filamentous ovules in the fourth whorl gynoecium of the Ap2-6 flower contribute to the partial sterility of Ap2-6 mutants. Both carpel–sepal and filamentous ovules may also form in the position of ovules on the first whorl organs of Ap2 mutant flowers (described below).

As shown in Figure 5F, the abnormal Ap2-6 ovules bear no resemblance to wild-type ovules in either morphology or cell surface features. In addition, the Ap2-6 carpel–sepal ovules are apparent by stage 13. Thus, in contrast to Bel1 ovules, the Ap2-6 carpel–sepal ovules develop early and do not appear to be derived specifically from the integument region.

The Ap2-6 ovule abnormalities segregate together with the other characteristics of the Ap2-6 mutant phenotype, suggesting that they are due to the *ap2-6* allele. In addition, abnormal ovules are not specific to the *ap2-6* allele because we have observed similar defects in another strong allele of *AP2* mutant, *ap2-7*.

Double Mutant Analysis

The phenotypic analysis of Bel1 and Ap2 mutants indicates that both genes play important roles in the morphogenesis of ovules in the fourth whorl of Arabidopsis flowers. We introduced the *bel1* mutation into plants homozygous for *ap2* and *ap3* and characterized the double mutant phenotypes for two reasons. First, *ap2* and *ap3* mutations result in ovule-bearing carpels in the first and third floral whorls, respectively (Bowman et al., 1989; Kunst et al., 1989). Thus, the double mutant phenotype would allow us to determine if *BEL1* is required for development of ovules regardless of their position within a flower. Second, because both *BEL1* and *AP2* genes affect development of ovules, phenotypic analysis of the Bel1/Ap2-6 double mutants can be useful in determining the extent of gene interaction.

Putative double mutants were identified on the basis of a novel phenotype and were genetically confirmed, as described in Methods. The double mutant phenotypes are described below.

Bel1-3/Ap3

Flowers of plants homozygous for recessive mutations in *AP3* have sepal-like organs in the second whorl and carpelloid organs in the third whorl. Depending on the *ap3* allele and growth conditions, the mutant phenotype varies in degree of third whorl carpelloidy (Bowman et al., 1989, 1991b). Ap3-1 flowers grown at 22°C have six stamen–carpel or carpel-like organs in the third whorl. In contrast, the stamen–carpel intermediate organs in the third whorl of Ap3-3 flowers are typically fused to the fourth whorl gynoecium (Bowman et al., 1991b). Figures 6A and 6B show that morphologically normal ovules can develop in the third whorl of Ap3-1 and Ap3-3 flowers, indicating that *ap3-1* and *ap3-3* have no obvious effect on ovule morphogenesis.

In Bel1-3/Ap3-1 and Bel1-3/Ap3-3 double mutant flowers, only abnormal Bel1-type ovules develop on the third whorl organs and within the gynoecium (Figures 6C and 6D). In the later stages of flower development (stage 17), the carpel-like structures characteristic for Bel1 mutants were observed in siliques of both double mutants. Therefore, the phenotype of both Bel1-3/Ap3-1 and Bel1-3/Ap3-3 double mutants indicated that the *BEL1* gene is required for normal ovule development in the third whorl carpels.

Bel1-3/Ap2-5

A weak *AP2* allele, *ap2-5*, causes sepal-to-carpel and petal-to-stamen transformations in the first and second whorls, respectively. As shown in Figure 7A, morphologically normal ovules develop on the first whorl sepal–carpel organs of Ap2-5 flowers. However, some of the structures developing in the position of ovules are not ovulelike. These unusual structures are carpel-like, judging from the cell surface features. In addition, they have one of two general morphologies that were described above for the gynoecium of Ap2-6 flowers: a carpel–sepal ovule or a thin filament often ending with stigmatic papillae. As shown in Figure 7B, the first whorl organs of a Bel1-3/Ap2-5 double mutant flower bear abnormal ovules typical for Bel1 and carpel–sepal ovules characteristic of Ap2. At stage 13 of flower development, the fourth whorl gynoecium of Bel1-3/Ap2-5 double mutant flowers contains Bel1-type ovules (Figure 7C), which occasionally develop into carpel-like structures typical for Bel1 by stage 17.

Bel1-3/Ap2-6

A strong *AP2* allele, *ap2-6*, causes sepal-to-carpel, petal-to-carpel, and occasionally stamen-to-carpel transformations and a reduction in organ number in the first three whorls (Kunst et al., 1989; E. Schultz and G.W. Haughn, unpublished observations). As shown in Figure 7D, the first and second whorls of an Ap2-6 flower are occupied by sepal–carpel organs bearing morphologically normal ovules, deformed ovulelike

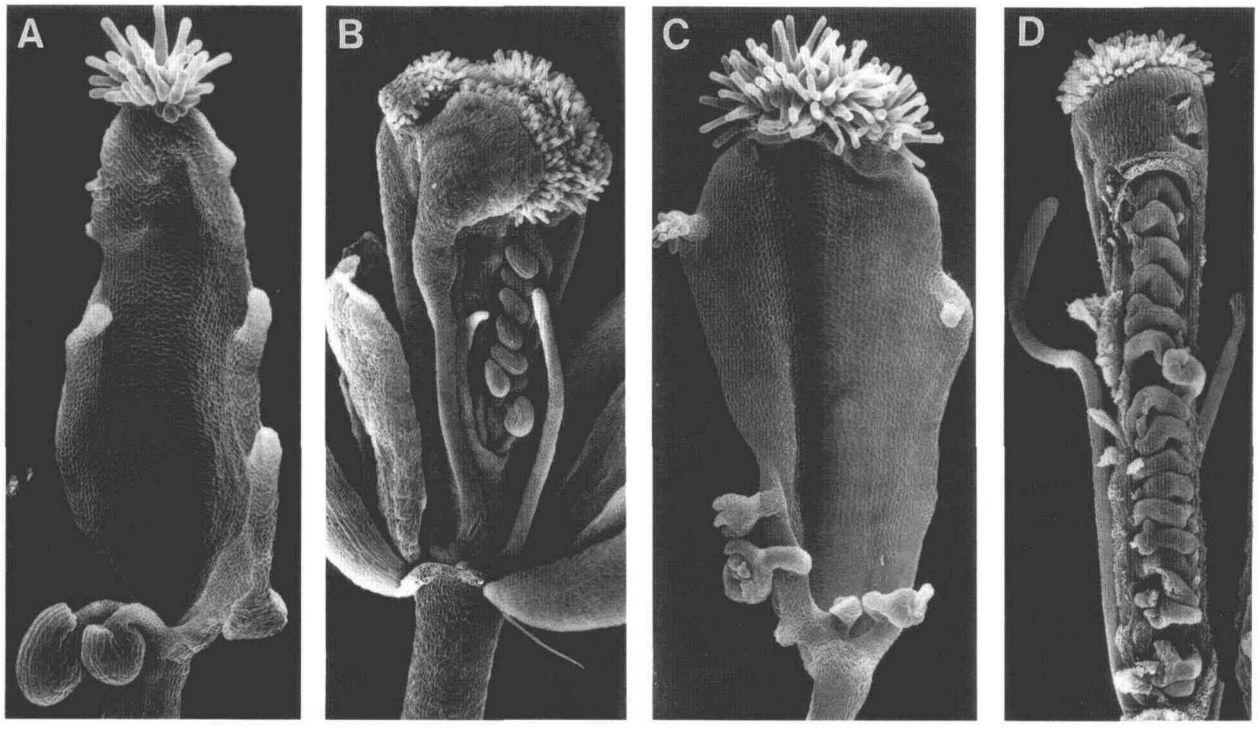

Figure 6. Scanning Electron Micrographs of Stage 13 Flowers from Ap3 Mutants and Bel1-3/Ap3 Double Mutants.

(A) Single carpel-like organ with normal ovules from the third whorl of an Ap3-1 flower. Magnification ×102.
(B) Ap3-3 flower with perianth partially removed. Third whorl carpels fuse to the fourth whorl gynoecium, and morphologically normal ovules are apparent. Magnification ×53.
(C) Single carpel-like organ from the third whorl of Bel1-3/Ap3-1 double mutant flower. Bel1 ovules develop at the carpel margin. Magnification ×95.
(D) Dissected gynoecium of Bel1-3/Ap3-3 double mutant flower. Bel1 ovules develop within the gynoecium, and filaments arise from the third floral whorl (perianth removed). Magnification ×72.

structures, carpel–sepal ovules, and filaments. The first whorl organs of Bel1-3/Ap2-6 double mutant flowers never bear morphologically normal ovules, and abnormal ovule types characteristic of Bel1 and Ap2 were frequently observed (Figure 7E). The fourth whorl organs of Bel1-3/Ap2-6 double mutant flowers typically have both Bel1-type ovules and a class of novel carpelloid ovules (Figure 7F). These novel carpelloid ovules are distinct from either Ap2-6 carpel–sepal ovules or Bel1 carpel-like structures. They usually have a flat, leaflike shape, are larger in size than either Bel1 or Ap2-6 abnormal ovules, and are comprised of cells whose irregular shape and surface features bear a strong resemblance to ovary cells. Differentiation of other cell types typical of Bel1 carpel-like structures and Ap2-6 carpel-sepal ovules, such as stigmatic papillar and sepaloid cells, respectively, have never been observed on these carpelloid ovules.

To determine whether the novel phenotype was specific to the Bel1-3/Ap2-6 double mutant and not due to other differences in genetic background, we crossed wild type (Columbia) × Bel1-3 (Wassilewskija) and wild type (Wassilewskija) × Ap2-6 (Columbia). The novel ovule morphology of Bel1-3/Ap2-6 double mutants was not observed among the progeny of either cross.

Together, double mutant analysis of the *bel1-3* allele and alleles of homeotic genes *AP3* and *AP2* suggested that the *BEL1* gene is required for development of morphologically normal ovules in all four whorls of the Arabidopsis flower. Further, the novel carpelloid ovule observed in the Bel1-3/Ap2-6 double mutant suggested that *BEL1* and *AP2* function independently in the ovule.

AG and *AP3* Gene Expression in *Bel1* Mutant Ovules

The floral organ identity genes *AG* and *AP3* are transcribed in wild-type Arabidopsis ovules (Bowman et al., 1991a; Jack et al., 1992). Because *bel1* mutations interrupt ovule development and cause homeotic transformation of outer integuments into carpel-like structures, we wanted to determine the effect of the *bel1* mutation on spatial distribution of *AG* and *AP3* transcripts. Figure 8 shows the results of in situ hybridization

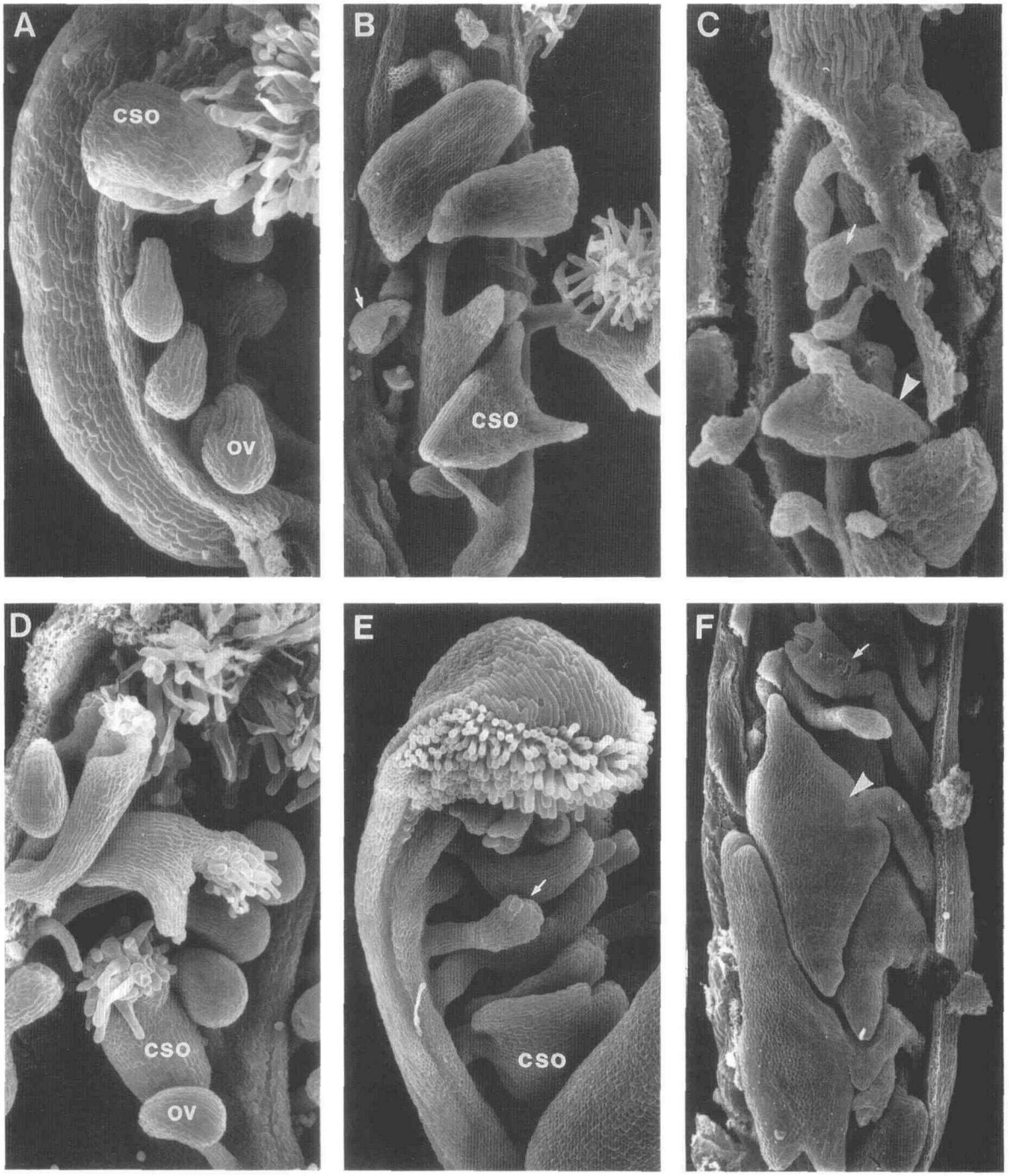

Figure 7. Scanning Electron Micrographs of Stage 13 Flowers of Ap2 Mutants and Bel1-3/Ap2 Double Mutants.

Structures are given the following abbreviations: ovule, ov; carpel–sepal ovules, cso.

(A) Sepal–carpel organ from the first whorl of Ap2-5 flower. At the margins, normal ovules and carpel–sepal ovules develop. Magnification ×137.

(B) Portion of a sepal–carpel organ from the first whorl of a Bel1-3/Ap2-5 double mutant flower. The arrow indicates a degenerating Bel1 ovule. Magnification ×85.

(C) Upper part of a dissected Bel1-3/Ap2-5 double mutant gynoecium. The arrow indicates the Bel1 ovule; the arrowhead indicates the developing carpel-like structure. Magnification ×162.

(D) Portion of a sepal–carpel organ from the first whorl of an Ap2-6 flower. Morphologically normal ovules and several developing carpel–sepal ovules are apparent. Magnification ×107.

(E) Sepal–carpel organ from the first whorl of a Bel1-3/Ap2-6 double mutant flower. The arrow indicates developing Bel1 ovule. Magnification ×120.

(F) Dissected gynoecium of a Bel1-3/Ap2-6 double mutant flower exhibiting a few Bel1 ovules (arrow) and a novel ovule type distinct in morphology and cell structure from either Ap2-6 carpel–sepal ovules or the Bel1 carpel-like structures (arrowhead). Magnification ×85.

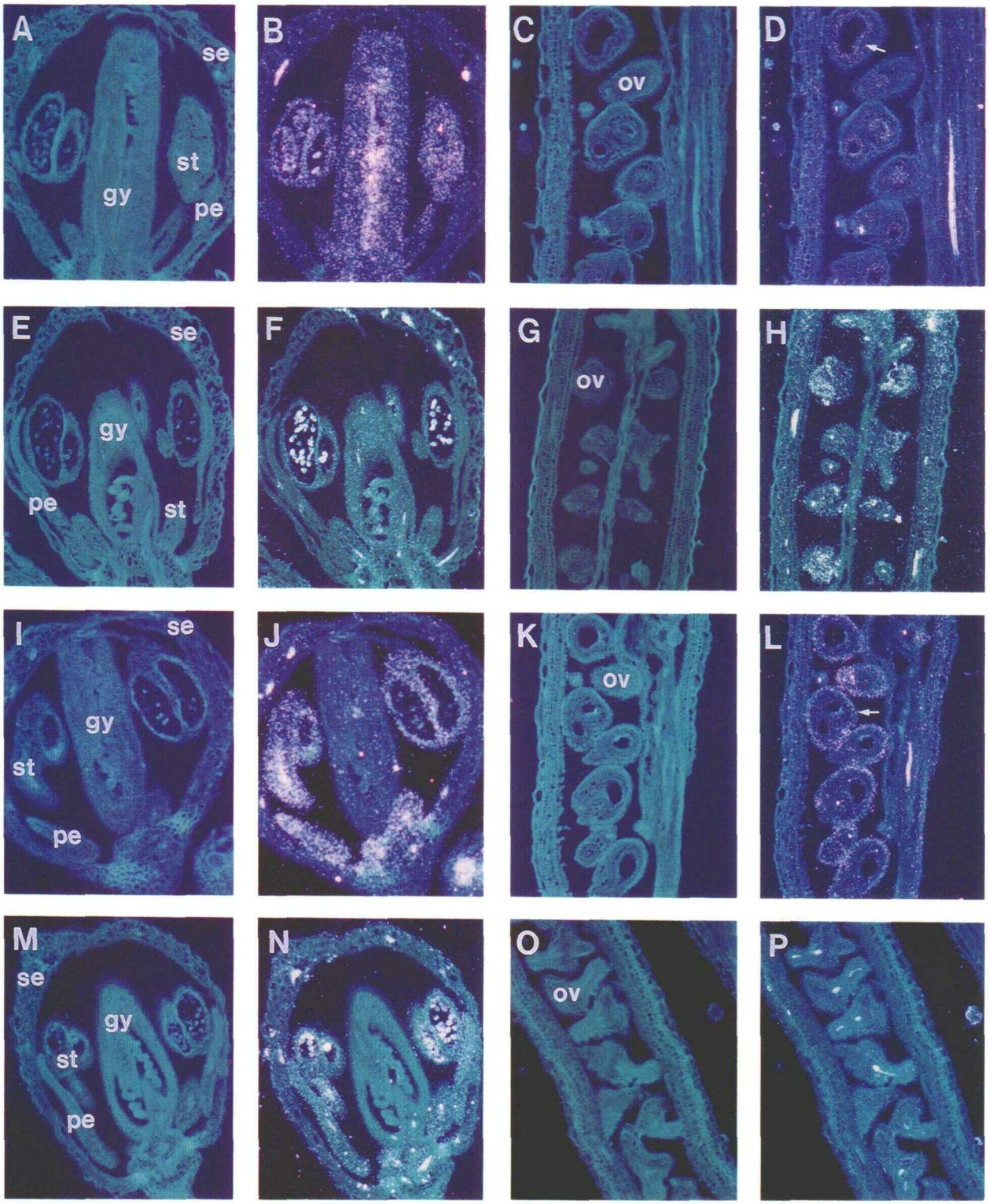

Figure 8. *AG* and *AP3* RNA Distribution in Wild-Type and Bel1 Flowers and Ovules.

The distribution of *AG* and *AP3* transcripts in wild-type and Bel1 flowers during different stages of flower development is shown. Each section was photographed in two ways: epifluorescence exposure **(A, C, E, G, I, K, M,** and **O)** and epifluorescence–dark-field double exposure **(B, D, F, H, J, L, N,** and **P)**. All flowers are oriented with the floral apex upward. Flower structures are given the following abbreviations: sepals, se; petals, pe; stamens, st; gynoecium, gy; ovule, ov.

(A) and **(B)** In situ hybridization of an *AG* antisense RNA probe with a stage 11 wild-type flower. Magnification ×173.

analyses in wild-type and Bel1-3 ovules using *AP3* and *AG* antisense RNAs as probes.

In agreement with earlier studies (Bowman et al., 1991a), *AG* was transcribed in the ovule primordia of stage 11 wild-type flowers (Figures 8A and 8B) and was limited to the endothelium of mature ovules (Figures 8C and 8D). In stage 11 Bel1-3 flowers (Figures 8E and 8F), the distribution of *AG* transcripts was not obviously different from that of wild-type flowers. However, at the time when *AG* expression in wild-type ovules was limited to the endothelium, *AG* transcripts were detected throughout the Bel1-3 ovules (Figures 8G and 8H; compare 8D to 8H). Thus, the *bel1-3* mutation results in ectopic *AG* expression late in ovule development.

AP3 gene transcripts were not detected in either wild-type or Bel1-3 developing ovules early in flower development (Figures 8I, 8J, 8M, and 8N; stages 10 and 11). By stage 13, mature wild-type ovules showed strong *AP3* expression that was limited to cells of the outer integument (Figures 8K and 8L). These results showed that the *AP3* gene is an excellent marker for normal development of the outer integument. In Bel1-3 mutant ovules in which morphologically normal outer integuments do not develop, *AP3* transcripts were barely detectable (Figures 8O and 8P). Although low levels of AP3 transcript may be present in Bel1-3 ovules, the level of expression was not equal to that observed in the outer integument of wild-type ovules (compare Figure 8L to 8P). At the cellular level, these results confirmed that normal outer integuments do not form in Bel1 mutant ovules.

DISCUSSION

Bel1 Gene Is Required for Ovule Development

Genetic mapping of the *bel1* mutation showed that *BEL1* represents a novel genetic locus that is distinct from other loci known to affect morphogenesis (Figure 2). All three mutant alleles of the *BEL1* gene that have been characterized to date (*bel1-1*, Robinson-Beers et al., 1992; *bel1-2* and *bel1-3*, Modrusan et al., 1994b; this study) are recessive and cause similar defects in ovule morphogenesis. Therefore, we assume that these mutations represent loss-of-function alleles.

Several general conclusions concerning the function of *BEL1* can be drawn on the basis of the single and double mutant phenotypes. First, *BEL1* is necessary for ovule development, regardless of the floral whorl in which the ovule appears (Figures 6C, 7B, and 7E). This suggested that the action of *BEL1* is subordinate to carpel formation. Second, *BEL1* does not appear to be required for the initiation of ovule primordia and early development of ovules, because the ontogeny of Bel1 ovules is normal until the time of integument initiation (Figures 3C and 3F). Third, normal integuments are not found in Bel1 ovules, indicating that *BEL1* is required for integument development (Figure 3T). One possibility is that the *BEL1* gene may play a specific, direct role in development of integuments. Alternatively, the *BEL1* gene may be needed for ovule development to progress beyond stage 10 and thus, may have an indirect influence on the development of integuments. Cloning of the *BEL1* gene and determining its spatial expression within ovules will help to distinguish between these alternatives. Fourth, the *BEL1* gene product plays a role in embryo sac development. Arrested megagametogenesis was observed in all sectioned Bel1 ovules (Figure 4H). This defect could be a pleiotropic effect resulting from the absence of integuments, or the *BEL1* gene may have a more direct role in the development of the female gametophyte.

BEL1 Negatively Regulates Class C Organ Identity Gene Expression Late in Ovule Development

An intriguing aspect of the Bel1 phenotype is the development of carpel-like structures from stage 13 Bel1 ovules (Figure 5). Clearly, ovule cells can be directed to follow the developmental program of an entire floral organ.

The formation of carpels during flower development in Arabidopsis is dependent on expression of the class C organ identity gene *AG*. In wild-type ovules, the *AG* gene is expressed throughout the ovule until stage 13, at which transcripts become restricted to the endothelium of the inner integuments (Figure 8D; Bowman et al., 1991a). However, in stage 13 Bel1-3 flowers, *AG* continues to be expressed throughout the ovule (Figure 8H), suggesting that the *BEL1* gene is involved in the negative regulation of *AG* expression in stage 13 wild-type ovules. Because ectopic expression of class C genes can direct both floral organ primordia outside the fourth whorl (Drews et al., 1991; Bradley et al., 1993) and ovule primordia (Mandel et al., 1992) to develop into structures with carpel-like features,

Figure 8. (continued).

(C) and **(D)** In situ hybridization of an *AG* antisense RNA probe with mature wild-type ovules. The arrow indicates the endothelium. Magnification ×194.
(E) and **(F)** In situ hybridization of an *AG* antisense RNA probe with a stage 11 Bel1-3 flower. Magnification ×131.
(G) and **(H)** In situ hybridization of an *AG* antisense RNA probe with developed Bel1-3 ovules. Magnification ×187.
(I) and **(J)** In situ hybridization of an *AP3* antisense RNA probe with a stage 10 wild-type flower. Magnification ×187.
(K) and **(L)** In situ hybridization of an *AP3* antisense RNA probe with mature wild-type ovules. The arrow indicates the outer integument where *AP3* expression is observed. Magnification ×147.
(M) and **(N)** In situ hybridization of an *AP3* antisense RNA probe with stage 11 Bel1-3 flower. Magnification ×139.
(O) and **(P)** In situ hybridization of an *AP3* antisense RNA probe with developed Bel1-3 ovules. Magnification ×194.

it seems reasonable to suggest that the Bel1 carpel-like structures are a result of the abnormal expression of the *AG* gene in the Bel1 ovule.

Although *BEL1* acts in ovules at least as early as stage 10 (Figure 3I), the negative regulation of *AG* by *BEL1* is not apparent until much later (stage 17; Figures 5B to 5E and 8D). How does the role of *BEL1* early in ovule development relate to its effect on the expression of *AG* late in ovule development? One possibility is that the *BEL1* gene product directly regulates *AG* throughout ovule development but that changes in transcript levels are obvious only by stage 13. In this way, all aspects of the Bel1 phenotype could be explained by uncontrolled *AG* expression. Alternatively, the relationship between *BEL1* and the regulation of *AG* could be indirect. The ectopic expression of *AG* in the Bel1 mutant might be a pleotropic effect of arresting the ovule early in development. Finally, the *BEL1* gene might have two distinct roles, one early in ovule development and one late.

The development of carpel-like structures is variable such that only some ovules on some plants possess these structures. Moreover, the frequency of carpel-like structures per silique and per plant is influenced by environmental conditions and genetic background. Interestingly, the environmental conditions that favor development of carpel-like structures (long photoperiods and high temperatures) also promote flower development in general (for a review, see Martinez-Zapater et al., 1994). Furthermore, of the three ecotypes examined, the one that flowers the earliest, namely Landsberg *erecta* (Martinez-Zapater et al., 1994), is also the one that has the highest frequency of carpel-like structures. Together, these data suggested that development of carpel-like structures is dependent on the strength of the floral inductive signal. A similar correlation between floral inductive conditions and the degree of carpelloidy observed in several other Arabidopsis mutants with altered floral morphology has been attributed to the influence of inductive conditions on class C organ identity gene expression.

We suggest that the formation of carpel-like structures in Bel1 mutants depends on the level of expression of *AG*, which can vary from ovule to ovule. Therefore, conditions that tend to increase *AG* expression (floral inductive conditions) also promote formation of carpel-like structures.

AP2 Gene Is Involved in Ovule Morphologenesis

The role of the *AP2* gene in perianth organ development (Komaki et al., 1988; Bowman et al., 1989, 1991b; Kunst et al., 1989) and in the initiation of flower development (Irish and Sussex, 1990; Shannon and Meeks-Wagner, 1993; Schultz and Haughn, 1993) has been well studied. The *AP2* gene is also required for normal development of the reproductive organs (Komaki et al., 1988; Kunst et al., 1989; Bowman et al., 1991b; Schultz et al., 1991). Formation of distinct carpel–sepal and filamentous ovules within the Ap2-6 gynoecium described here suggests that *AP2* has a role in ovule development. This hypothesis is supported by the fact that *AP2* expression has been observed in wild-type ovules (J. Okamuro, personal communication).

Abnormal Ap2-6 ovules do not resemble wild-type ovules either in cell surface features or morphology, although both of them appear to develop during the same period of flower development (Figure 5F). Thus, as in floral organ development, *AP2* seems to function relatively early in ovule development. The variability in structure of the Ap2-6 ovule makes the exact role of the *AP2* gene difficult to ascertain. However, the carpel-like features of the abnormal Ap2-6 ovules suggested that the *AP2* gene is involved in regulating the expression of *AG* early in ovule development. This hypothesis is consistent with the known role of *AP2* in inhibiting expression of *AG* in the outer two whorls during flower development (Kunst et al., 1989; Bowman et al., 1991b; Drews et al., 1991).

Morphologically normal ovules are also found in the Ap2-6 gynoecium (Figure 5F). Sufficient *AP2* activity may remain in the Ap2-6 mutant to permit normal development of some ovules. Alternatively, the role of the *AP2* gene in the wild-type plant may be to limit the choice of the ovule primordium to a single developmental program. If the latter hypothesis were true, the absence of *AP2* activity in Ap2-6 would permit the ovule primordium to commit to one of several fates, only one of which is that of normal ovule development.

An important question concerns the relationship of *AP2* and *BEL1* function during ovule development. The fact that a novel ovule type was observed in the Bel1-3/Ap2-6 gynoecium indicated that *BEL1* is expressed in the Ap2-6 ovules and that *AP2* is expressed in Bel1 ovules. Therefore, the expression of *AP2* in ovules does not appear to depend on *BEL1* expression and vice versa. Beyond this conclusion, a comparison of the single and double mutant phenotypes revealed few general trends. For example, the novel type of carpelloid ovule observed in Bel1-3/Ap2-6 double mutants cannot be described as more carpel-like than those of Ap2-6 or Bel1; therefore, it is difficult to speculate on the relative contributions of *BEL1* and *AP2* with respect to the negative regulation of the carpel program during ovule development.

Role of Organ Identity Genes in Wild-Type Ovule Development

Floral organ identity in the Arabidopsis flower is specified by the combination of three classes of genes, with overlapping domains of expression in the floral shoot (Coen and Meyerowitz, 1991). As discussed above, the class A gene *AP2* appears to play a role in ovule development. In addition, ectopic expression of class C genes clearly has effects on ovule development (Mandel et al., 1992; this study). By contrast, the role of a class B gene, *AP3*, during wild-type ovule development is not known. Hybridization experiments showed that the *AP3* and *AG* genes are transcribed in very specific subsets of cells of developed wild-type ovules (Figures 8D and 8L). Moreover, the position of the *AP3* expression in the stage 13

ovule, relative to that of *AG*, is analogous to what is seen in the early floral meristem. Despite these observations, it appears that morphologically normal ovules can develop in the absence of the *AP3* and *AG* gene expression. That is, morphologically normal ovules were observed in Ap3 mutants (Figures 6A and 6B) and occasionally in Ag/Ap2 double mutants (Bowman et al., 1989). If indeed the organ identity genes play a role in ovule morphogenesis, then either their role is a subtle one or there is enough functional redundancy to allow normal ovule development even in their absence.

BEL1 Influences Inflorescence Structure

Mutations in *BEL1* result in the termination of the apical meristem of the primary shoot in a pistil-like structure. Analogous inflorescence abnormalities have been observed in the male-sterile mutant Ms1-1 (T. Bleecker, personal communication), Leafy mutants (Huala and Sussex, 1992; Schultz and Haughn, 1993), and transgenic Arabidopsis plants in which *AG* is controlled by the cauliflower mosaic virus (CaMV) 35S promoter (Mizukami and Ma, 1992). In the latter two cases, the inflorescence defects have been attributed to ectopic expression of *AG* in the primary meristem (Mizukami and Ma, 1992; Schultz and Haughn, 1993). *BEL1* and *MS1* may also influence the expression of *AG* in inflorescence meristems, although it seems unlikely that they do so directly. The only other characteristic that Bel1 and Ms1 mutant plants have in common is sterility. It is conceivable that sterility influences the strength of the floral inductive process which in turn affects development of the primary shoot (Schultz and Haughn, 1993). Information concerning the inflorescence structure of a wide variety of sterile plants could help to test such a hypothesis.

Developmental Potential of the Ovule

The ovule phenotypes seen in Bel1 and Ap2-6 demonstrated that substructures of an organ have the potential to follow the developmental program of the floral organ from which they are derived. Such flexibility in developmental potential is not limited to Arabidopsis. In tobacco, placental tissues of wild-type and methylglyoxal *bis*-(guanylhydrazone)–resistant mutants 3 (Mgr3) and 9 (Mgr9) cultured in vitro develop carpelloid structures in place of the ovule (Evans and Malmberg, 1989). Similar carpelloid ovules were caused by ectopic expression of an oilseed rape *AG*-like gene in tobacco (Mandel et al., 1992). These observations illustrate an aspect of complexity underlying the control of morphogenesis. Genes, such as *AG*, that are involved in establishing organ type must initiate subprograms that direct development of substructures, such as the ovule. However, once activated, genes specific to the subprogram must replace the organ identity genes as the primary regulators of morphogenesis. An understanding of the molecular events of such regulatory interactions during floral morphogenesis remains an important goal.

METHODS

Plant Material, Growth Conditions, and Genetic Methods

Two *Arabidopsis thaliana* (ecotype Wassilewskija) lines segregating for the Bell1 (Bel1) phenotype, Female-sterile (Fms = Bel1-2) and Fruitless (Fts = Bel1-3), were isolated from a collection of independent lines transformed with *Agrobacterium tumefaciens* (Feldmann, 1991). The Bel1-1 mutant line isolated from an ethyl methanesulfonate–mutagenized population of Arabidopsis (ecotype Landsberg *erecta*) has been described recently (Robinson-Beers et al., 1992). Before being used for the analyses reported here, both mutant alleles, *bel1-2* and *bel1-3*, were back-crossed three times to the wild type. All Bel1 mutants were maintained as heterozygotes and analyzed within F_2-segregating populations. Lines used for genetic mapping were W100 (Landsberg *erecta*, *an*, *ap1*, *er*, *py*, *hy2*, *gl1*, *bp*, *cer2*, *ms1*, *tt3*; Koornneef et al., 1987), and TC 35 (Columbia × Landsberg *erecta*, *yi*, *pgm*, *ttg*; gift from T. Caspar, Central Experimental Station, Du Pont, Wilmington, DE). Lines used for construction of double mutants were Ap2-5, Ap2-6 (Kunst et al., 1989), Ap3-1 (gift from M. Koornneef, Department of Genetics, Wageningen Agricultural University, The Netherlands), and Ap3-3 (gift from E. Meyerowitz, California Institute of Technology, Pasadena, CA).

Routinely, plants were grown at 22°C under continuous fluorescent illumination (Gro-Lux; Sylvania) at 80 to 120 $\mu E\ m^{-2}\ sec^{-1}$ photosynthetically active radiation (PAR) on Terra-lite Redi-earth (W.R. Grace & Co. Canada Ltd., Ajax, Ontario). Other photoperiodic regimes (16-hr illumination, 100 to 150 $\mu E\ m^{-2}\ sec^{-1}$ PAR; 10-hr illumination, 150 to 180 $\mu E\ m^{-2}\ sec^{-1}$ PAR) and other temperatures (16°C) were used as indicated.

For genetic mapping of *BEL1*, recombination frequencies were determined by analyzing F_2 progenies using the method of Suiter et al. (1983).

DNA Isolation and Gel Blot Analysis

Genomic DNA was isolated from either Bel1-2 or Bel1-3 mutant plants as described by Dellaporta et al. (1983), digested with either AvaI or HindIII, resolved in an 0.8% agarose gel, transferred onto a nitrocellulose membrane (BA45; Schleicher & Schuell), and labeled with random hexamers (Boehringer-Mannheim). The neomycin phosphotransferase II (*NPTII*) probe encoding kanamycin resistance was gel purified from plasmid pDO421 (gift from D. Ow, Plant Gene Expression Center, Albany, CA). After hybridization and washing, the filter was exposed to Kodak XAR-5 film.

Light and Scanning Electron Microscopy

For light microscopy, floral buds were fixed in FAA (50% ethanol, 5% glacial acetic acid, 3.7% formaldehyde) with 1% Triton X-100 at 4°C for at least 3 days. Samples were rinsed several times in 50% ethanol, dehydrated through a graded ethanol series, and stained in 100% ethanol containing 1% safranin for easier orientation of the material. Tissue was infiltrated with a mixture of 100% ethanol and JB4 Plus (Polysciences, Warrington, PA) embedding resin (ratios 3:1, 1:1, and 1:3), followed by three changes of pure resin. Blocks were polymerized overnight at room temperature. Sections were cut 2 to 3 μm thick with a tungsten carbide knife on a micron microtome and stained with

0.05% aqueous toluidine blue. Photographs were taken with T-MAX 100 film on a microscope (Axiophot; Zeiss).

For scanning electron microscopy, flowers at different stages of development were vacuum infiltrated with 3% glutaraldehyde in 0.02 M sodium phosphate buffer, pH 7.2, and fixed overnight at 4°C. The samples were rinsed several times in buffer, and the youngest floral stages were postfixed in OsO_4 in the same buffer for 2 hr. All samples were dehydrated in a graded acetone series before being critical point dried in liquid carbon dioxide and mounted on stubs. In some instances, perianth organs were removed from flowers, and pistils were then dissected with pulled glass needles. Stubs with prepared material were coated with gold in a sputter coater (model S150B; Edwards, Grand Island, NY) and examined with a scanning electron microscope (model 505; Philips, Eindhoven, The Netherlands) at an accelerating voltage of 30 kV.

Construction of Double Mutants

Bel1-3 plants were crossed to plants homozygous for the *APETALA* alleles *ap2-5*, *ap2-6*, *ap3-1*, and *ap3-3*. The double mutants were identified and verified for each cross as follows:

bel1-3/ap2-5 and bel1-3/ap2-6

Among the F_2 progeny of Bel1-3 × Ap2-5 and Bel1-3 × Ap2-6 crosses, four phenotypes were found in a ratio of 388 wild type to 142 Ap2-5 to 135 Bel1-3 to 42 with the novel phenotype (9:3:3:1, $\chi^2 = 1.06$, $P > 0.5$) and 104 wild type to 35 Ap2-6 to 24 Bel1-3 to 8 with the novel phenotype (9:3:3:1, $\chi^2 = 7.76$, $P > 0.05$), respectively. To confirm that the novel phenotype represented the double mutant, we allowed F_2 progeny with the Ap2 phenotype that was representative of each cross to self. In the case of 10 Ap2-5 plants, five segregated for a novel phenotype in a ratio of 328 Ap2-5 to 104 (3:1, $\chi^2 = 0.20$, $P > 0.5$). In the case of 10 Ap2-6 plants, four segregated for the novel phenotype in a ratio of 82 Ap2-6 to 21 (3:1, $\chi^2 = 0.012$, $P > 0.9$). Four putative Bel1-3/Ap2-5 F_2 plants and three putative Bel1-3/Ap2-6 F_2 plants were shown to be homozygous for *ap2-5* (*ap2-6*) and *bel1-3* by testcrossing to ap2-5/ap2-5 (ap2-6/ap2-6) and Bel1-3/bel1-3 plants. Several Ap2-5 and Ap2-6 plants among the F_1 progeny from the crosses Ap2-5/Bel1-3 × Ap2-5 or Ap2-6/Bel1-3 × Ap2-6, respectively, were allowed to self, and double mutants Ap2-5/Bel1-3 or Ap2-6/Bel1-3 among their F_1 progeny were used for phenotypic analysis.

bel1-3/ap3-1 and bel1-3/ap3-3

Among the F_2 progeny of crosses Ap3-1 × Bel1-3 and Ap3-3 × Bel1-3, a novel phenotype with characteristics of both Bel1-3 and Ap3 was observed. Phenotypes in the F_2 generation were in a ratio of 252 wild type to 73 Ap3-1 to 65 Bel1-3 to 21 Ap3-1/Bel1-3 (9:3:3:1, $\chi^2 = 4.78$, $P > 0.1$) and 233 wild type to 80 Ap3-3 to 72 Bel1-3 to 22 Ap3-3/Bel1-3 (9:3:3:1, $\chi^2 = 0.93$, $P > 0.5$). Because both Bel1-3/Ap3-1 and Bel1-3/Ap3-3 double mutants were male and female sterile, we were unable to perform further genetic analysis on these plants, and phenotypic analysis was conducted on the putative double mutants from the F_2 generation.

In Situ Hybridization

Young inflorescences were fixed by vacuum infiltration with 4% paraformaldehyde in 0.1 M phosphate buffer, pH 7.0, for 16 hr at 4°C. Fixed tissue was rinsed twice in the same buffer, dehydrated with ethanol, cleared with a mixture of ethanol and xylene (ratios 2:1 and 1:2 [v/v]) followed by pure xylene, and then embedded in paraffin (Paraplast Plus; Sigma). Serial sections (5 to 10 μm) were attached to gelatin-coated slides, deparaffinized in xylene, and rehydrated in a series of decreasing ethanol concentrations. Subsequent pretreatment of slides for in situ hybridization, time and temperature of hybridization, and post-hybridization treatment were conducted as described by Huijser et al. (1992). After standard autoradiographic procedures, slides were stained with 0.01% fluorescent brightener 28 (calcofluor white; Sigma). The distribution of grains and the underlying tissue were examined using a combination of dark-field illumination and UV fluorescence.

The *AGAMOUS* (*AG*) and *AP3* antisense RNA probes were constructed by linearizing plasmid pCIT565 with HindIII or plasmid pD793 with BglII and transcribing in vitro with T7 RNA polymerase as described previously (Yanofsky et al., 1990; Jack et al., 1992). The RDEF49 antisense probe used as a negative control was generated by transcribing pDH49 (RDEF49 cDNA in the pBluescript KS+ vector) with T7 RNA polymerase. RDEF49 is a MADS box gene transcribed in ovules of *Antirrhinum majus* (Z. Schwarz-Sommer, unpublished results). No hybridization to Arabidopsis ovules was detected.

ACKNOWLEDGMENTS

This work was supported by a Natural Sciences and Engineering Research Council of Canada (NSERC) Research Grant to G.W.H., a University of Saskatchewan postgraduate scholarship to Z.M., a National Science Foundation (NSF) Research Fellowship (No. IBN-9304998) to R.L.F., and a NSF Center for Plant Developmental Biology Fellowship (No. DIR-8719933) to L.R. The contribution of the Central Research and Development Department of Du Pont de Nemours and Co. in making their transformed lines available for screening is gratefully acknowledged. We thank Drs. Ljerka Kunst, Alon Samach, and Elizabeth Schultz for critical reading of the manuscript; Drs. Hans Sommer, Zsuzsanna Schwarz-Sommer, Peter Huijser, and Patrick Motte for help with in situ hybridization analysis; Dr. Elliot Meyerowitz for providing plasmids pCIT565 and pD793; Dr. David Ow for providing the pDO421 plasmid; Dr. Steve Ruzin for helpful suggestions; Chad Williams for excellent technical assistance; and Drs. Tony Bleecker, Zsuzsanna Schwarz-Sommer, and Jack Okamuro for communicating unpublished data.

Received November 10, 1993; accepted January 27, 1994.

REFERENCES

Bowman, J.L., Smyth, D.R., and Meyerowitz, E.M. (1989). Genes directing flower development in *Arabidopsis*. Plant Cell **1**, 37–52.

Bowman, J.L., Drews, G.N., and Meyerowitz, E.M. (1991a). Expression of the Arabidopsis floral homeotic gene *AGAMOUS* is restricted to specific cell types late in flower development. Plant Cell **3**, 749–758.

Bowman, J.L., Smyth, D.R., and Meyerowitz, E.M. (1991b). Genetic interactions among floral homeotic genes of *Arabidopsis*. Development **112**, 1–20.

Bradley, D., Carpenter, R., Sommer, H., Hartley, N., and Coen, E. (1993). Complementary floral homeotic phenotypes result from opposite orientations of a transposon at the *plena* locus in Antirrhinum. Cell **72**, 85–95.

Coen, E.S., and Meyerowitz, E.M. (1991). The war of the whorls: Genetic interactions controlling flower development. Nature **353,** 31–37.

Dellaporta, S.L., Wood, J., and Hicks, J.B. (1983). A plant DNA minipreparation: Version II. Plant Mol. Biol. Rep. **1,** 19–22.

Drews, G.N., Bowman, J.L., and Meyerowitz, E.M. (1991). Negative regulation of the *Arabidopsis* gene *AGAMOUS* by the *APETALA2* product. Cell **65,** 991–1002.

Evans, P.T., and Malmberg, R.L. (1989). Alternative pathways of tobacco placental development: Time and commitment and analysis of a mutant. Dev. Biol. **136,** 273–283.

Feldmann, K.A. (1991). T-DNA insertion mutagenesis of *Arabidopsis*: Mutational spectrum. Plant J. **1,** 71–82.

Guignard, J.L., Agier, C., and Bury, M. (1991). Developpement de l'embryon zygotique chez l'*Arabidopsis thaliana* Schur. Bull. Soc. Bot. Fr. **138,** 149–154.

Huala, E., and Sussex, I.M. (1992). *LEAFY* interacts with floral homeotic genes to regulate Arabidopsis floral development. Plant Cell **4,** 901–913.

Huijser, P., Klein, J., Lönnig, W.-E., Meijer, H., Saedler, H., and Sommer, H. (1992). Bracteomania, an inflorescence anomaly, is caused by the loss of function of the MADS-box gene *squamosa* in *Antirrhinum majus*. EMBO J. **11,** 1239–1249.

Irish, V.F., and Sussex, I.M. (1990). Function of the *apetala-1* gene during *Arabidopsis* floral development. Plant Cell **2,** 741–753.

Jack, T., Brockman, L.L., and Meyerowitz, E.M. (1992). The homeotic gene *APETALA3* of *Arabidopsis thaliana* encodes a MADS box and is expressed in petals and stamens. Cell **68,** 683–697.

Komaki, M.K., Okada, K., Nishino, E., and Shimura, Y. (1988). Isolation and characterization of novel mutants of *Arabidopsis thaliana* defective in flower development. Development **104,** 195–203.

Koornneef, M., Hanhart, C.J., van Loenen-Martinet, E.P., and van der Veen, J.H. (1987). A marker line that allows the detection of linkage on all *Arabidopsis* chromosomes. Arabidopsis Info. Serv. **23,** 46–50.

Kunst, L., Klenz, J.E., Martinez-Zapater, J., and Haughn, G.W. (1989). *AP2* gene determines the identity of perianth organs in flowers of *Arabidopsis thaliana*. Plant Cell **1,** 1195–1208.

Mandel, M.A., Bowman, J.L., Kempin, S.A., Ma, H., Meyerowitz, E.M., and Yanofsky, M.F. (1992). Manipulation of flower structure in transgenic tobacco. Cell **71,** 133–143.

Mansfield, S.G., and Briarty, L.G. (1991). Early embryogenesis in *Arabidopsis thaliana*. II. The developing embryo. Can J. Bot. **69,** 461–476.

Mansfield, S.G., Briarty, L.G., and Erni, S. (1991). Early embryogenesis in *Arabidopsis thaliana*. I. The mature embryo sac. Can. J. Bot. **69,** 447–460.

NOTE ADDED IN PROOF

Similar results concerning conversion of ovules into carpels and ectopic expression of *AG* RNA in Bel1 mutants have been observed by Ray et al. (1994).

Ray, A., Robinson-Beers, K., Ray, S., Baker, S.C., Lang, J.D., Pruess, D., Milligan, S.B., and Gasser, C.S. (1994). The *Arabidopsis* floral homeotic gene *BELL* controls ovule development through negative regulation of *AGAMOUS*. Proc. Natl. Acad. Sci. USA, in press.

Martinez-Zapater, J.M., Coupland, G., Dean, C., and Koornneef, M.K. (1994). The transition to flowering in *Arabidopsis*. In *Arabidopsis*, E.M. Meyerowitz and C. R. Somerville, eds (Cold Spring Harbor, NY: Cold Spring Harbor Laboratory Press), in press.

Misra, R.C. (1962). Contribution to the embryology of *Arabidopsis thalianum* (Gay & Monn.). Univ. J. Res., Agra **11,** 191–198.

Mizukami, Y., and Ma, H. (1992). Ectopic expression of the floral homeotic gene *AGAMOUS* in transgenic *Arabidopsis* plants alters floral organ identity. Cell **71,** 119–131.

Modrusan, Z., Reiser, L., Fischer, R., and Haughn, G.W. (1994a). Ontogeny of the *Arabidopsis* wild type ovule. In *Arabidopsis*: An Atlas of Morphology and Development, J. Bowman, ed (New York: Springer-Verlag), pp. 302–303.

Modrusan, Z., Reiser, L., Fischer, R., Feldmann, K.A., and Haughn, G.W. (1994b). Bel1 mutants are defective in ovule development. In *Arabidopsis*: An Atlas of Morphology and Development, J. Bowman, ed (New York: Springer-Verlag), pp. 304–305.

Robinson-Beers, K., Pruitt, R.E., and Gasser, C.S. (1992). Ovule development in wild-type Arabidopsis and two female-sterile mutants. Plant Cell **4,** 1237–1249.

Schultz, E.A., and Haughn, G.W. (1993). Genetic analysis of floral initiation process (FLIP) in *Arabidopsis*. Development **119,** 745–765.

Schultz, E.A., Pickett, F.B., and Haughn, G.W. (1991). The *FLO10* gene product regulates the expression domain of homeotic genes *AP3* and *PI* in Arabidopsis flowers. Plant Cell **3,** 1221–1237.

Shannon, S., and Meeks-Wagner, D.R. (1993). Genetic interactions that regulate inflorescence development in Arabidopsis. Plant Cell **5,** 639–655.

Smyth, D.R., Bowman, J.L., and Meyerowitz, E.M. (1990). Early flower development in *Arabidopsis*. Plant Cell **2,** 755–767.

Suiter, K.A., Wendel, J.F., and Case, J.S. (1993). LINKAGE-1: A PASCAL computer program for the detection and analysis of genetic linkage. J. Hered. **74,** 203–204.

Velten, J., and Schell, J. (1985). Selection-expression plasmid vectors for use in genetic transformation of higher plants. Nucl. Acids Res. **13,** 6981–6998.

Webb, M.C., and Gunning, B.E.S. (1990). Embryo sac development in *Arabidopsis thaliana*. 1. Megasporogenesis, including the microtubular cytoskeleton. Sex. Plant Reprod. **3,** 244–256.

Webb, M.C., and Gunning, B.E.S. (1991). The microtubular cytoskeleton during development of the zygote, proembryo and free-nuclear endosperm in *Arabidopsis thaliana* (L.) Heynh. Planta **184,** 187–195.

Yanofsky, M.F., Ma, H., Bowman, J.L., Drews, G.N. Feldmann, K.A., and Meyerowitz, E.M. (1990). The protein encoded by the *Arabidopsis* homeotic gene *AGAMOUS* resembles transcription factors. Nature **346,** 35–40.